not a necessary step in the coalescence reaction. It is more likely a channel for release of excess energy from apparently thermodynamically favorable reactions.

These results also suggest that formation of the higher fullerene ions from cyclo[18]carbon is surprisingly efficient. The pathway to these ions evidently includes C_{70}^+ (but not C_{60}^+), because the major peaks have the formula $C_{(70\ +\ 18n)}$, rather than simply C_{18m}^+ as do those below m/z 840. Thus the larger fullerene ions appear to form through sequential ion/molecule (C_x^+/C_{18}) reactions. Surprisingly, C_{70}^+ appears to undergo addition of a C_{18} unit as readily as the higher fullerenes from the observation of similar ratios of C_{70}^+/C_{88}^+ and C_{88}^+/C_{106}^+.

Laser desorption of **2** (Fig. 1B) yields similar results to that of **1**. Again, C_{70}^+ is the major product with further addition of C_{24} units leading to higher fullerene ions. However, more C_2 loss accompanies these coalescence reactions than in the case of **1**. This result is consistent with the expected higher exothermicity of incorporating an additional six carbon atoms into the fullerene for C_{24} versus C_{18} addition.

A laser desorption mass spectrum of **3** is shown in Fig. 1C. In this case, no C_{30}^+ is observed and C_{60}^+ is the major product ion. The extensive amount of C_2 loss observed in this spectrum confirms the expectation that the coalescence of C_{30}^+ with a neutral C_{30} to form a C_{60}^+ ion is likely to be very exothermic. Further addition of C_{30} units to C_{60}^+, C_{58}^+, and so forth yields higher fullerene ions through both coalescence with C_{30} and loss of C_2. However, although C_{60}^+ is by far the most abundant ion, C_{90}^+ is less abundant than C_{88}^+, C_{86}^+, and so forth. Thus, in contrast to the reaction of C_{70}^+ with C_{18} and C_{24} discussed above, it appears that C_{60}^+ reacts by addition of C_{30} much more slowly than do the fragmentation products (C_{58}^+, C_{56}^+, and so forth) which can account for its high relative abundance.

These results conclusively demonstrate that one reaction pathway to the formation of fullerenes is the coalescence of large cyclocarbon species. These studies with molecular precursors also show that the distribution of fullerenes can be directly affected by the properties, such as size, of these precursors. Insight into formation mechanisms as described and the use of molecular precursors (in contrast to graphite) should ultimately lead to the ability to control the size distribution of both fullerenes and fullerene derivatives, such as metallofullerenes, that are formed in growth processes.

REFERENCES AND NOTES

1. F. W. McLafferty, Ed., *Acc. Chem. Res.* **25**, 98–175 (1992).
2. W. Krätschmer *et al.*, *Nature* **347**, 354 (1990).
3. J. M. Hawkins *et al.*, *J. Am. Chem. Soc.* **113**, 9394 (1991); T. W. Ebbesen *et al.*, *Chem. Phys. Lett.* **191**, 336 (1992).
4. J. R. Heath, *ACS Symp. Ser.* **481**, 161 (1992).
5. R. F. Curl and R. E. Smalley, *Sci. Am.* **265**, 32 (April 1991).
6. H. W. Kroto, A. W. Allaf, S. P. Balm, *Chem. Rev.* **91**, 1213 (1991).
7. D. H. Robertson, D. W. Brenner, C. T. White, *J. Phys. Chem.* **96**, 6133 (1992).
8. S. C. O'Brien, J. R. Heath, R. F. Curl, R. E. Smalley, *J. Chem. Phys.* **88**, 220 (1988).
9. T. Wakabayashi and Y. Achiba, *Chem. Phys. Lett.* **190**, 465 (1992).
10. T.-M. Chang *et al.*, *J. Am. Chem. Soc.* **114**, 7603 (1992).
11. M. Broyer *et al.*, *Chem. Phys. Lett.* **198**, 128 (1992).
12. G. v. Helden, M.-T. Hsu, P. R. Kemper, M. T. Bowers, *J. Chem. Phys.* **95**, 3835 (1991).
13. F. Diederich *et al.*, *Science* **245**, 1088 (1989).
14. F. Diederich and Y. Rubin, *Angew. Chem. Int. Ed. Engl.* **31**, 1101 (1992).
15. Y. Rubin *et al.*, *J. Am. Chem. Soc.* **113**, 495 (1991).
16. H. So and C. L. Wilkins, *J. Phys. Chem.* **93**, 1184 (1989); C. E. Brown *et al.*, *J. Polym. Sci: Part A: Polym. Chem.* **26**, 131 (1988); W. R. Creasy, and J. T. Brenna, *Chem. Phys.* **126**, 453 (1988); D. N. Lineman *et al.*, *J. Phys. Chem.* **93**, 5025 (1989); P. F. Greenwood *et al.*, *Fuel* **69**, 257 (1990).
17. Experiments were performed on the Fourier transform ion cyclotron resonance mass spectrometer (FTMS) located at the Naval Research Laboratory as described in (*20*). Laser desorption was performed with the focused output (10^7 to 10^8 W/cm^2) of a pulsed CO_2 laser operating at 10.6 μm. Laser spot sizes were estimated to be 100 to 500 μm^2. Solutions of the carbon oxides in dichloromethane were deposited onto stainless steel probe tips which, following evaporation of the solvent, were inserted into the vacuum system.
18. J. A. Zimmerman, J. R. Eyler, S. B. H. Bach, S. W. McElvany, *J. Chem. Phys.* **94**, 3556 (1991).
19. S. W. McElvany, B. I. Dunlap, A. O'Keefe, *ibid.* **86**, 715 (1987); S. W. McElvany, *ibid.* **89**, 2063 (1988).
20. D. C. Parent and S. W. McElvany, *J. Am. Chem. Soc.* 111, 2393 (1989).
21. C. Yeretzian *et al.*, *Nature* **359**, 44 (1992).

22. We acknowledge the Office of Naval Research for financial support of this work and the National Science Foundation for a predoctoral fellowship (to N.S.G.). We also thank H. Guard for helpful discussions, J. Milliken and Y. Rubin for assistance in synthetic procedures, and H. Nelson and A. Baronavski for assistance with the CO_2 laser.

3 November 1992; accepted 21 January 1993

An Inorganic Double Helix: Hydrothermal Synthesis, Structure, and Magnetism of Chiral $[(CH_3)_2NH_2]K_4[V_{10}O_{10}(H_2O)_2(OH)_4(PO_4)_7]\cdot 4H_2O$

Victoria Soghomonian, Qin Chen, Robert C. Haushalter,* Jon Zubieta,* Charles J. O'Connor

Very complicated inorganic solids can be self-assembled from structurally simple precursors as illustrated by the hydrothermal synthesis of the vanadium phosphate, $[(CH_3)_2NH_2]K_4[V_{10}O_{10}(H_2O)_2(OH)_4(PO_4)_7]\cdot 4H_2O$, 1, which contains chiral double helices formed from interpenetrating spirals of vanadium oxo pentamers bonded together by P^{5+}. These double helices are in turn intertwined with each other in a manner that generates unusual tunnels and cavities that are filled with $(CH_3)_2NH_2^+$ and K^+ cations, respectively. The unit cell contents of dark blue phosphate 1, which crystallizes in the enantiomorphic space group $P4_3$ with lattice constants a = 12.130 and c = 30.555 angstroms, are chiral; only one enantiomorph is present in a given crystal. Magnetization measurements show that 1 is paramagnetic with ten unpaired electrons per formula unit at higher temperatures and that antiferromagnetic interactions develop at lower temperatures.

Organic materials have been synthesized that can self-assemble into ordered arrays at low temperature, that are capable of molecular recognition, and that can act as biomimetic systems (*1*). Corresponding advances in synthetic inorganic chemistry have lagged behind the organic areas primarily because of the unavailability of suitable molecular precursors. Small, soluble molecular building blocks with well-defined reaction chemistries that would allow their low-temperature assembly into crystalline solid state inorganic materials are not well known. However, it is clear from the study of many naturally occurring, structurally complex mineral species that hydrothermal synthesis (*2*) can provide a low-temperature pathway to produce open framework, metastable structures utilizing solid-state inorganic starting materials. Similar hydrothermal conditions have been used to synthesize microporous tetrahedral framework solids that are capable of shape-selective absorption, like the zeolites and aluminophosphates (*3*).

Recently, hydrothermal syntheses were used to prepare microporous, octahedral-tetrahedral framework molybdenum phosphates (*4*). These materials represent the

V. Soghomonian, NEC Research Institute, 4 Independence Way, Princeton, NJ 08540, and Department of Chemistry, Syracuse University, Syracuse, NY 13244.
Q. Chen and J. Zubieta, Department of Chemistry, Syracuse University, Syracuse, NY 13244.
R. C. Haushalter, NEC Research Institute, 4 Independence Way, Princeton, NJ 08540.
C. J. O'Connor, Department of Chemistry, University of New Orleans, New Orleans, LA 70148.

*To whom correspondence should be addressed.

beginning steps toward solid-state materials that would combine the shape-selective absorptivities of a zeolite with the thermal stability and reactive transition element site of a catalytically active metal oxide. A common and usually necessary feature of many microporous solids is the presence of a cationic organic template which, being larger than inorganic cations, can leave a micropore large enough to sorb molecules when removed from the framework. Although vanadium phosphates have been prepared with metal cation templates in the framework voids (*5–12*), no examples of the direct incorporation of organic templates during synthesis were known. We report the hydrothermal synthesis, single-crystal x-ray structure, and magnetic properties of $[(CH_3)_2NH_2]K_4[V_{10}O_{10}(H_2O)_2(OH)_4(PO_4)_7]\cdot 4H_2O$, **1**, which contains chiral, interpenetrating double helices built up from vanadium phosphate units.

Hydrothermal treatment of KVO_3, V, H_3PO_4, $CH_3PO(OH)_2$, $(CH_3)_2NH$, and H_2O in a mole ratio of 2.35:1:10.18:3.31:8:1137 for 4 days at 200°C gives greater than 85% yield of monophasic, dark blue tetragonal bipyramids of **1**. It is not only surprising that the very complex structure of **1** is self-assembled from such structurally simple starting materials, but that it is formed in quantitative yield. These optimized synthetic conditions were determined empirically after the observation of **1** in other reactions with the same starting materials but with different mole ratios. Although the role of the methylphosphonic acid is not known and it is not incorporated into the product, it is crucial to the high yield synthesis of **1** under these conditions.

The structure of **1** was determined by single-crystal x-ray diffraction (*13*) and consists of a three-dimensional covalently bonded framework built up from VO_6 octahedra, VO_5 square pyramids, and PO_4 tetrahedra. Phosphate **1** crystallizes in the space group $P4_3$ (or its enantiomorph $P4_1$), and therefore the crystals are enantiomorphic and the unit cell contents are chiral. The fundamental building blocks are two structurally similar, crystallographically independent vanadium oxo pentamers, one of which is shown in Fig. 1. Although each pentamer may appear to possess $\bar{1}$ symmetry, examination of the V–O distances shows that actually there is no symmetry present because of the alternation of long V–O (~2.4 Å) and short V=O (~1.7 Å) contacts along the seven-atom central V–O backbone of the pentamer. This backbone has a short V=O bond at one end and a long V–O bond to an H_2O ligand at the other. The pentamers have a V–O–V backbone containing four V–O–V and two V–OH–V bonds. The connectivity is such that there is a central trimer of three VO_6 octahedra, with the central octahedron sharing *trans* corners with the two outer octahedra. Each of two outer octahedra of the trimer share an edge with two VO_5 square pyramids (Fig. 1). These pentamers are arranged so as to form spirals, with four pentamers per spiral of unit cell length along [001].

The spirals in turn are intertwined to give the two strands of a double helix as shown in Fig. 2A with one strand composed of V1–V5 and the other strand V6–V10. These helices are very unusual in that the two directions parallel to the axis of the helix are inequivalent and, because of the tetragonal space group, the helices appear to have a square cross section when viewed in projection down [001]. The perpendicular distance of the V–O backbone within the spiral to the central axis of the spiral varies as a function of the z coordinate of the unit cell, which results in what appears to be protruding major and minor loops when the helix is viewed from various angles perpendicular to the spiral axis (Fig. 2B). There are seven different types of P^{5+} cations in the unit cell. Some P^{5+} atoms serve to join the pentamers and some to connect the strands to one another to form the helix, whereas others bond one double helix to another.

These strands and double helices intergrow with one another in an extremely complicated fashion, as is illustrated schematically in Fig. 3. The essence of the symmetry is represented by the two sets of five unique V atoms and P1. The loops protruding from each double helix are quite large. Within a given unit cell, portions of the two crystallographically independent strands of each double helix undergo an excursion into the adjacent unit cells on either side of the original unit cell and then turn 90° and form the minor loop before returning to a point one unit cell translation in c away but with the same x and y coordinates. When the helix forms the largest loops, another strand from another helix goes through the open loop. This interweaving of the strands and helices gives rise to a three-dimensional array of interconnected braids.

This connectivity of the covalently bonded vanadium phosphate framework generates cavities and a topologically unusual array of tunnels that contain the K^+ and $(CH_3)_2NH_2^+$ cations, respectively. As

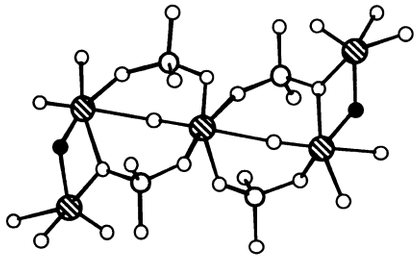

Fig. 1. One of the two crystallographically independent pentameric vanadium oxo building blocks present in **1**. The pentamer, which is held together by four V–O–V and two V–OH–V (μ^2–OH groups black) bonds as well as phosphate bridges, possesses no symmetry because of the alternation of long V–O and short V=O bonds along the backbone. These pentamers are bonded together by additional P^{5+} centers to form the covalent three-dimensional framework.

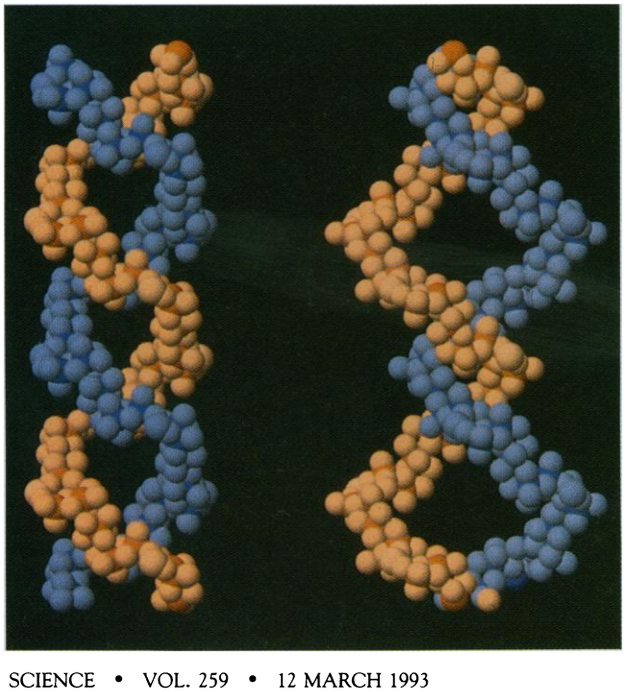

Fig. 2. Two of the crystallographically independent vanadium oxo spirals that interpenetrate to form one of the double helices found in **1**. The different colored spirals are bonded together with P^{5+} (not shown). Both views are perpendicular to [001]: (**A**) view down [1$\bar{1}$0] and (**B**) view down [100] showing the major and minor loops that correspond to excursions of the strands radially from the main axis of the spiral. Spirals such as these two intertwine with additional helices to form the three-dimensional structure of **1**.

shown in Fig. 4, A and B, which are projections of the unit cell contents parallel to the tetragonal *a* and *b* axes, respectively, the tunnels that are filled with the dimethylammonium cations run parallel both to [100] at 1/4 and 3/4 in *c* and parallel to [010] at 0 and 1/2 but at no point do the two types of tunnel intersect. In fact, the atoms that are the "ceiling" of one tunnel form the "floor" of the perpendicular tunnel above it. Note that the shorter contacts of the less polar organic cations to the framework are the vanadyl (V=O) groups. The K^+ cations lie in more polar regions of the structure and are coordinated to the solvate water. We previously speculated, based on the observations in several molybdenum phosphates (*4*, *14*) in which nonpolar organic cations were associated with less polar molybdenyl (Mo=O) regions of the framework and polar inorganic cations (such as Na^+, NH_4^+, and H_3O^+) were near the phosphate regions of the framework, that hydrophobic-hydrophilic interactions are an important factor in understanding how these mixed organic-inorganic systems crystallize.

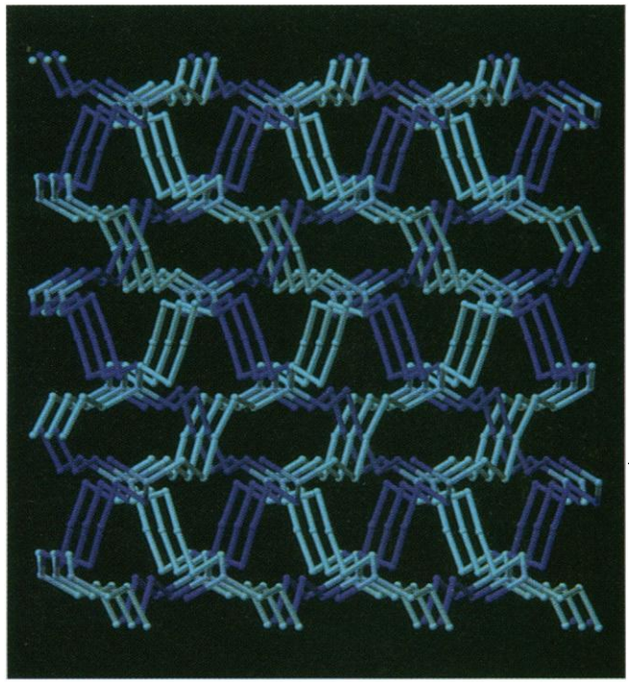

Fig. 3. A simplified illustration of how the spirals and double helices intertwine with one another. The essence of the symmetry is represented by the ten vanadium atoms, with each of the two sets of crystallographically independent V atoms represented with different colors, and P1.

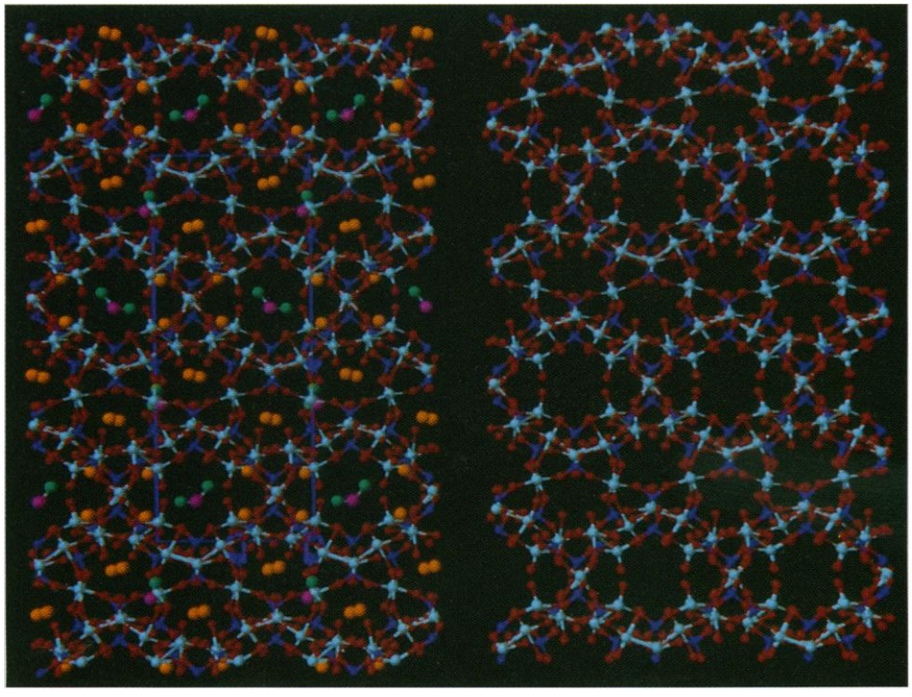

Fig. 4. Projection of the unit cell contents of **1** (**A**) down [100] and (**B**) [010] where the tunnels that are filled with the $(CH_3)_2NH_2^+$ cations can be seen. In (B), all of the cations are removed to emphasize the voids in the anionic framework. The two views are displayed with the same *z* coordinates to emphasize how the tunnels lie in parallel planes but run at 90° relative to one another. Note that the "ceilings" and "floors" of one set of tunnels form the floors and ceilings, respectively, of the two adjacent tunnels which run at 90°. The water solvate molecules are not shown. Color key: V, light blue; P, dark blue; O, red; K, yellow; C, aqua; and N, magenta.

Investigation of the magnetic properties of **1** shows that at room temperature there are ten unpaired electrons per V_{10} formula unit, a result consistent with the bond strength–bond length calculations (*15*), and the characteristic square pyramidal or distorted octahedral geometry of the vanadium, both of which indicate all ten V are d^1 V^{4+}. At lower temperatures, there is a decrease in the magnetic moment of **1**, from 1.63 μ_B per V at room temperature to 1.01 μ_B at 2.5 K, because of low-dimensional antiferromagnetic interactions. We have not yet been able to model the interactions successfully.

The preparation of an open framework vanadium phosphate synthesized with organic templates that displays chirality suggests several areas of additional research. The tunnels in which the $(CH_3)_2NH_2^+$ cations reside are not exactly cylindrical, and the atoms responsible for the minimum constrictions of ~6.9 and 8.1 Å (atom-to-atom distances) do not define planes that are perpendicular to the axis of the tunnel. Although we have not yet measured the sorption properties of **1**, some of the V atoms have potentially removable aquo ligands and it may be possible to observe shape-selective absorption into a solid with vacant coordination sites on a transition element in solids like **1**. In principle, one could envision absorption or catalysis that would discriminate between enantiomers. Because **1** is a rare example of a material that is both chiral and strongly magnetic, it may provide an opportunity to see if any interactions exist between polarized light and an internal or external magnetic field.

REFERENCES AND NOTES

1. J. S. Lindsey, *New J. Chem.* **15**, 153 (1991).
2. A. Rabenau, *Angew. Chem. Int. Ed. Engl.* **24**, 1026 (1985).
3. R. M. Barrer, *Hydrothermal Chemistry of Zeolites* (Academic Press, New York, 1982); D. W. Breck, *Zeolite Molecular Sieves* (Krieger, Malabar, FL, 1974); R. Szostak, *Molecular Sieves: Principles of*

Synthesis and Identification (Van Nostrand Reinhold, New York, 1989); M. L. Occelli and H. E. Robson, *Zeolite Synthesis* (American Chemical Society, Washington, DC, 1989).
4. For a review, see R. C. Haushalter and L. A. Mundi, *Chem. Mater.* **4**, 31 (1992).
5. $Zn_2VO(PO_4)_2$: K. H. Lii and H. J. Tsai, *J. Solid State Chem.* **90**, 291 (1991).
6. $Cs_2V_3P_4O_{17}$: K. H. Lii, Y. P. Wang, S. L. Wang, *ibid.* **80**, 127 (1989).
7. β-$K_2V_3P_4O_{17}$: K. H. Lii, H. J. Tsai, S. L. Wang, *ibid.* **87**, 396 (1990).
8. $A_2VOP_2O_7$ (A=Cs, Rb): K. H. Lii and S. L. Wang, *ibid.* **82**, 239 (1989).
9. AVP_2O_7 (A = Li-Cs): K. H. Lii, Y. P. Wang, Y. B. Chen, S. L. Wang, *ibid.* **86**, 143 (1990) and references therein.
10. $NaVOPO_4$: K. H. Lii, C. H. Li, T. M. Chen, S. L. Wang, *Z. Kristallogr.* **197**, 67 (1991).
11. $RbV_3P_3O_{17+x}$: K. H. Lii, C. S. Lee, *Inorg. Chem.* **29**, 3298 (1990).
12. A. V. Lavrov, V. P. Nikolaev, G. G. Sadikov, M. A. Porai-Koshits, *Sov. Phys. Dokl.* **27**, 680 (1982).
13. Crystal data for **1**: tetragonal, space group $P4_3$ (no. 78) with a = 12.130(2) and c = 30.555(5) Å at 25°C with Z = 4, V = 4495.8(14) Å^3, and $R(R_w)$ = 0.0477(0.0509).
14. R. C. Haushalter and F. W. Lai, *Angew. Chem. Int. Ed. Engl.* **28**, 743 (1989).
15. I. D. Brown and D. Altermatt, *Acta. Crystallogr. B* **41**, 244 (1985).
16. The work at Syracuse University was supported by NSF grant CHE9119910. The coordinates have been deposited at the Fachinformationszentrum Karlsruhe, Gesellschaft für wissenshaftlich-technische Informationen mbH, D-W-7514 Eggenstein-Leopoldshafen 2, Germany.

20 November 1992; accepted 26 January 1993

Fullerenes from a Fulgurite

Terry K. Daly, Peter R. Buseck,* Peter Williams, Charles F. Lewis

Peaks at 720 and 840 atomic mass units were identified by mass spectrometry in a sample extracted from a fulgurite, which is a glassy rock that forms where lightning strikes the ground. The peaks are interpreted as arising from C_{60} and C_{70} and the associated peaks as produced from other fullerenes. The intense conditions generated by the lightning not only melted the rock it struck and fused the associated soil but also allowed fullerenes to form, presumably from the organic debris in the soil.

Fullerenes (C_{60} and C_{70}) were first identified in products from laser ablation experiments (*1*). They were subsequently synthesized with the use of carbon arcs (*2*, *3*), combustion (*4*, *5*), and ion beams (*6*), all under intense conditions that rarely occur in the natural environment. However, fullerenes were recently reported from a geological sample (*7*). In that report, Buseck *et al.* speculated that lightning strikes might provide extreme conditions that could resemble those used for the laboratory synthesis of fullerenes. Therefore, we decided to investigate fulgurites, the geological products of lightning, for the presence of natural fullerenes.

Lightning produces a wide variety of unusual effects, one of which is that the ground area where the lightning strikes tends to melt. The peculiar branching forms produced in this way commonly have dendritic structures reminiscent of the stepped leaders of lightning. The resulting fulgurites typically consist of glass, the result of the intense heat produced by the lightning. They are usually tubular, with hollow interiors and fragile, porous exteriors. The inner diameters of tubular fulgurites are generally in the millimeter to centimeter range, comparable to typical lightning channel diameters (*8*). Fulgurites contain phases that require temperatures exceeding 2000 K (*9*–*11*), reflecting the extreme conditions that can be produced locally by lightning.

We examined a variety of fulgurites derived from different materials and locations (Table 1). Portions of each sample were pulverized and placed into an extraction thimble that was then loaded into a clean Soxhlet apparatus. The samples were cycled in the Soxhlet system for 24 hours (toluene was used as the solvent) (*12*). All glassware was cleaned and baked after each extraction. Upon completion, the solvent was evaporated, and the extracts were redissolved in ~1 ml of distilled toluene. A droplet of the concentrated sample was placed onto a copper substrate for analysis by time-of-flight (TOF) mass spectrometry. The samples were desorbed from the copper surface by a 355-nm ultraviolet neodymium:yttrium-aluminum-garnet laser with an ~0.9-mJ, 8-ns pulse focused to ~0.5 mm^2. An accelerating voltage of +20 kV produced a TOF mass spectrum of positively charged ion fragments.

The fulgurite found on Sheep Mountain, Colorado, near Wolf Creek Pass (37°29′N, 106°54′W), contained detectable fullerenes; the others did not. The glass of the Sheep Mountain sample is black and vesicular along the outer parts of the tube. Figure 1 shows a portion of the fulgurite tube perched on top of the host rock from which it presumably formed. The fulgurite is fused to that rock, which also contains melted pockets within its bulk, clearly showing that the lightning caused extreme heating but only in highly localized regions. The black glass within the pockets (a few millimeters in diameter) is free of macroscopic vesicles and has the appearance of dense black obsidian. The centers of the larger pockets are hollow and so may indicate the existence of small glass tubes passing through the interior of the rock. They occur up to at least 5 cm from the fulgurite on the rock exterior.

Fig. 1. The fullerene-bearing fulgurite from Sheep Mountain. The tubular, glassy mass on top and the pockets within the rock were produced by lightning (a few millimeters across).

Table 1. Fulgurite samples studied.

Source material	Location	Source	Identification no.	Contains fullerenes?
Ash-flow tuff	Sheep Mountain, CO	Chuck Lewis		Yes
Quartz sand	Florida	U.S. National Museum	74118.0000	No
Quartz sand	Alamosa County, CO	David New		No
Glacial till	Winans Lake, MI	Eric Essene		No
Pseudofulgurite*	Maryland	U.S. National Museum	116544.0000	No

*This sample was produced when a broken high-power line fell to the ground.

T. K. Daly and P. Williams, Department of Chemistry and Biochemistry, Arizona State University, Tempe, AZ 85287.
P. R. Buseck, Department of Chemistry and Biochemistry and Department of Geology, Arizona State University, Tempe, AZ 85287.
C. F. Lewis, Center for Meteorite Studies, Arizona State University, Tempe, AZ 85287.

*To whom correspondence should be addressed.